ICES Journal of Marine Science, 59: 380–392. 2002
doi:10.1006/jmsc.2001.1174, available online at http://www.idealibrary.com on IDEAL®

Observations of the mass and flow field at Porcupine Bank

Christian Mohn, Joachim Bartsch, and Jens Meincke

Mohn, C., Bartsch, J., and Meincke, J. 2002. Observations of the mass and flow field at Porcupine Bank. – ICES Journal of Marine Science, 59: 380–392.

During spring 1994 and summer 1995 hydrographic transects across the Porcupine Bank, an elliptical topographic structure adjoining the shelf-edge west of Ireland, were carried out to investigate the thermohaline properties and flow field characteristics in the vicinity of the bank. The CTD observations show a dome-like deformation of the temperature and density field together with an intrusion of cold, dense water above the bank summit. Additional acoustic current measurements in summer 1995 indicate that the dome-like perturbation of the mass field is accompanied by an anti-cyclonic, bottom-intensified circulation along the flanks of the bank. The doming of the near-bank temperature and density field and the eddy-like pattern of the flow field in summer 1995 may result from a Taylor column formation. It is suggested that a persistent Taylor column circulation around Porcupine Bank provides an important mechanism for the retention of pelagic eggs and larvae of the various marine species spawning in the area.

Keywords: Porcupine Bank, Taylor column formation, tidal rectification.

Received 13 November 2000; accepted 15 November 2001.

C. Mohn: Alfred Wegener Institute for Polar and Marine Research, Bremerhaven, Germany. J. Bartsch: HYDROMOD – SEAMAR Project Office, Mittelfeldweg 18e, 27607 Langen, Germany. J. Meincke: Institute of Oceanography, Center for Marine and Climate Research, University of Hamburg, Germany. Correspondence to C. Mohn: Alfred Wegener Institute for Polar and Marine Research, Postfach 120161, 27515 Bremerhaven, Germany. Tel.: +49 (0)471 4831 1703; e-mail: cmohn@awi-bremerhaven.de and mohn@dkrz.de

Introduction

The investigation of the flow regime over seamounts has received growing attention during the past decade. Field observations on a number of isolated seamounts, including the Great Meteor Seamount in the North Atlantic (Meincke, 1971) and the Fieberling Guyot in the North Pacific (Kunze and Toole, 1997), identified dome-like deformations of the temperature and density field as well as substantial perturbations of the flow field in the vicinity of the seamount summit. From theoretical considerations the dynamics involved were interpreted as mechanisms based on the theory of Taylor column formation and the generation of freely-propagating trapped waves at isolated topographic features. Numerical studies at isolated seamounts with both idealized (Brink, 1990; Chapman and Haidvogel, 1992) and realistic topography (Beckmann and Haidvogel, 1997) showed that these processes lead to closed, anticyclonic re-circulations around the seamount. A number of geological and biological studies (e.g. Genin *et al*., 1986; Boehlert, 1988) suggest that seamount-related currents are an important factor in the distribution of fauna and sediments (Genin, 1989). An overview of comprehensively investigated seamounts is given by Rogers (1994). Near-shore banks, including Georges Bank off the east coast of North America (Loder *et al*., 1988) and Rockall Bank in the north-eastern North Atlantic (Dooley, 1984) have received special attention due to their importance for regional fisheries.

The present study focuses on the hydrographic investigation of the area surrounding Porcupine Bank based on CTD and acoustic current measurements. The observations were carried out in the framework of the EU/AIR funded project SEFOS (Shelf-Edge Fisheries and Oceanography Study). During different seasons between March 1994 and July 1995 the data were obtained along zonal transects through the Porcupine Bank area. The observations are supplemented by sea surface temperature (SST) satellite measurements. In this study the properties of the stratification and flow field in the central Porcupine Bank relative to its

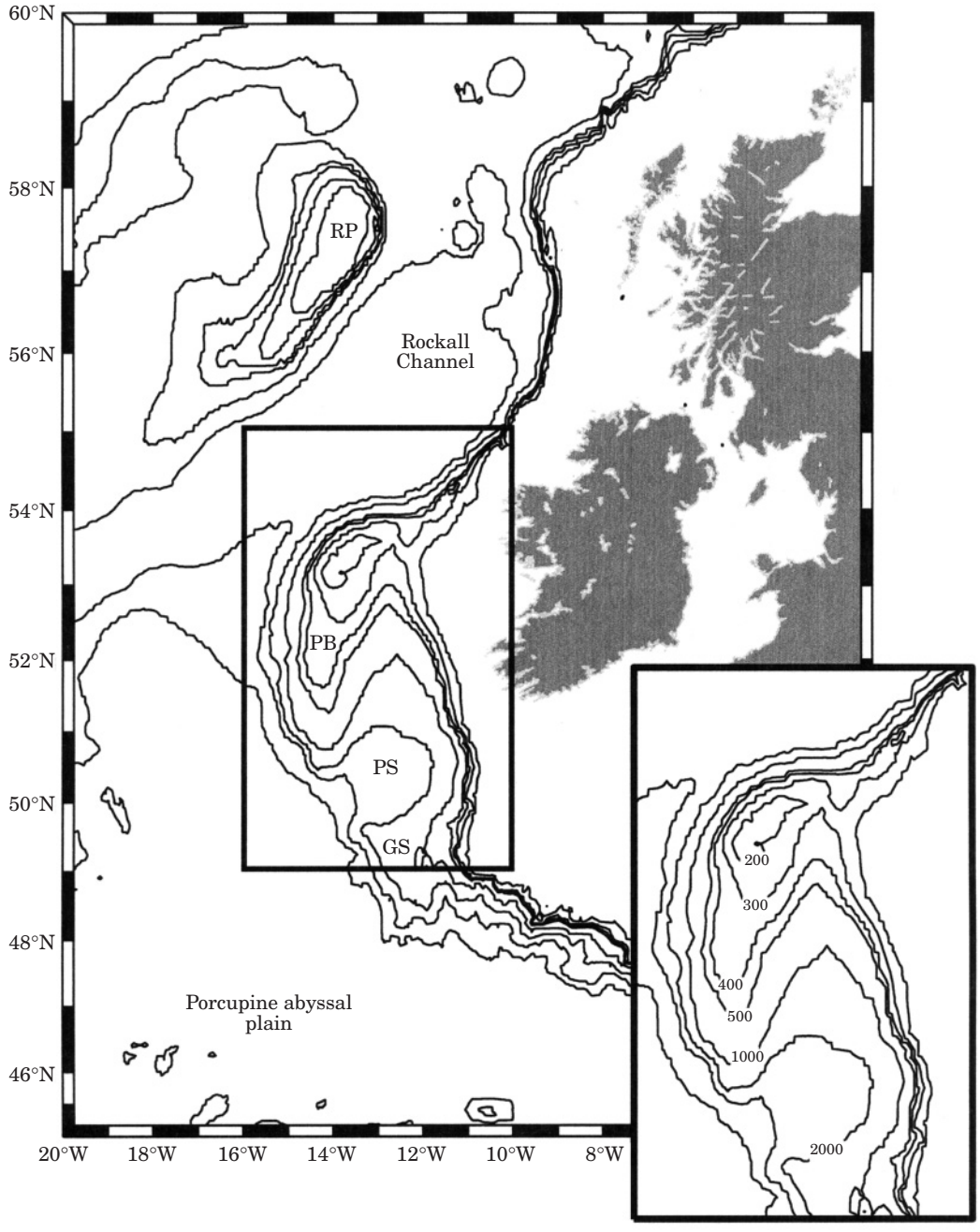

Figure 1. Map showing the Porcupine Bank region. Depth contours are in metres and geographical features are labelled PB (Porcupine Bank), PS (Porcupine Seabight) and GS (Goban Spur).

surroundings in summer 1995, are described and compared with hydrographic measurements in spring 1994. Dynamical aspects of the observed flow pattern are discussed with respect to results of recent numerical and field studies of flow in the vicinity of seamounts.

Materials and methods

The area of investigation covers the central Porcupine Bank, an elliptically-shaped topographic feature, situated at the north-west European shelf-edge west of Ireland (Figure 1). Its main axis is orientated essentially

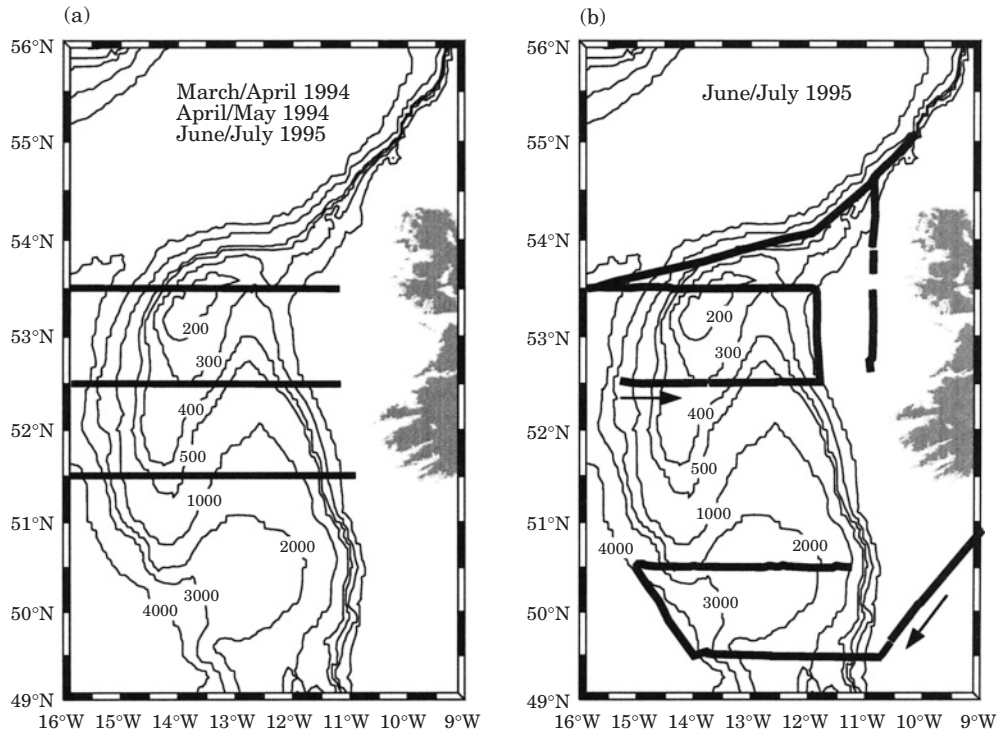

Figure 2. CTD transects (a) and ADCP cruise track (b) across the Porcupine Bank area. Depth contours are in metres.

in the north–south direction and rises to depths between 170 m and 500 m below the sea surface. The bank profile is marked by a strong east-west asymmetry. The western part of the bank falls into the northern Porcupine Abyssal Plain with a steep continental slope down to depths greater than 4000 m. To the east of the central bank plateau at 53.5°N there is no clear separation from the Irish shelf break; the bank slope is comparatively shallow with water depths not exceeding 300 m.

Three transects with almost identical station grids were surveyed across the Porcupine Bank area (see Figure 1(a)) by RV "Valdivia" (May 1994, July 1995) and RV "Heincke" (March 1994). At each station CTD casts were performed from the surface to near the bottom except for technical limitations. The CTD used in March 1994 allowed a maximum deployment depth of 1000 m, in July 1995 the maximum sampling depth was limited to 3000 m because of problems with the winch/wire system. Additional water samples were collected at up to 12 discrete depth levels using a rosette system. The bottle samples were analyzed for salinity, which was used for the calibration of the CTD data. WOCE standard accuracy was achieved (Mohn, 1999).

Continuous current measurements were performed during the RV "Valdivia" cruises using a ship-mounted Acoustic Doppler Current Profiler (ADCP) with an operating frequency of 153.6 kHz and a maximum depth of 480 m. The water velocity relative to the ship was recorded in depth intervals of 16 m during sampling intervals of 6 minutes. The May 1994 data were rejected due to malfunction of three of the four transducers. In July 1995 the data acquisition was split into two legs due to a 5-day gap in the acquisition procedure stemming from technical problems. The resulting data set was post-processed following the strategy and recommendations of the Common Oceanographic Data Access System (CODAS) of the University of Hawaii (Firing *et al.*, 1995). The cruise track is shown in Figure 2(b). The ADCP data were corrected for bad GPS fixes, misalignment of the transducer with the ship's keel and the effects of the Schuler-oscillation of the ship's gyro (Mohn, 1999). The misalignment of the transducer with the ship's keel leads to a bias of the Doppler shift determination and significantly limits the accuracy of absolute water velocities. The misalignment angle (φ) and the scaling factor (A) were estimated using the water track calibration method (Firing *et al.*, 1995), where all changes of ship speed and course during the cruise were selected. The selection criteria are based on reference values for the course change and the acceleration phase of the ship. A total of 150 estimates were used for the calibration. The estimations were performed separately for measurements before and after the interruption of data acquisition. The results yield $\varphi = -2.52 \pm 0.55$ and $A = 1.0039 \pm 0.021$ for the first leg and $\varphi = -0.77 \pm 0.43$ and $A = 1.0052 \pm 0.024$ for the second leg. Errors in the

determination of φ and A in the order of 0.6 and 1% cause errors in the absolute water velocities of 1% of the ship speed (Firing *et al*., 1995). Assuming a maximum ship speed of 6 m s^{-1} during the summer 1995 cruise, the resulting error from the water-track calibration is up to ± 5.5 cm s^{-1} for the first leg and ± 4.3 cm s^{-1} for the second leg. Only the data of the second leg are used in this study. A possible gyro-drift could not be verified, since an additional external navigation system was not available. The ADCP velocities refer to the entire oceanic motion, including longer periodic fluctuations, such as tides and inertial oscillations. The influence of the barotropic flow constituents is minimized by eliminating the dominant diurnal and semi-diurnal tidal signal from the summer 1995 ADCP data set with an harmonic function of the form:

$$u(t) = u_0 + \sum_{i=1}^{2} b_i \cos(\omega_i t) + c_i \sin(\omega_i t)$$

The coefficients b_i and c_i are of polynomial form

$$b_i(\phi,\lambda) = \sum_{j=1}^{3} \sum_{k=0}^{j} g_l \phi^{j-k} \lambda^k, l = (j-k,k)$$

where t is the time, ω_i is the frequency of the M_2 and K_1 tidal constituents, φ and λ are geographic coordinates and g_l are constant coefficients to be fitted to the observations. The polynomial form of c_i is according to b_i with constant coefficients h_l. The function is fitted to the vertically averaged horizontal velocity components u_0 in a least-square sense and then subtracted from the ADCP velocities. It takes into account the spatial variability of the tidal constituents. In order to get a statistically-independent time series in relation to the tidal motion all processed samples were used for analysis. This method was successfully applied by Candela *et al*. (1990) in the Yellow Sea and by Bersch (1995) in the northern North Atlantic.

Results

Temperature and density field

Figure 3 shows the lateral distribution of potential temperature Θ (°C) and potential density σ_0 (kg m^{-3}) on the 180 dbar isobar extracted from the CTD measurements. This isobar represents the depth level immediately above the Porcupine Bank summit and was chosen to describe the main features of water-mass properties at the bank and its surroundings. A recurring feature in the temperature and density distributions is a core of cold water of high density centered above the bank. In this area, a consistent relationship between temperature and density was observed during all sample periods. The density characteristics are mainly determined by temperature, since a corresponding pattern in the distribution of salinity (not presented here) was absent. To the west and east of the central bank area the cold core is enclosed by relatively warm water, which is transported northwards by the European Shelf-Edge Current (SEC) (Pingree and LeCann, 1990). From March to May 1994 (Figure 3(a–d)) the cold core extends over a relatively large area beyond the bank summit with persistent temperature and densities of Θ9.5°C and $\sigma_0 \geq 27.34$ kg m^{-3}, respectively. The stability of the core properties indicates that there was no, or limited, exchange of water masses between the bank area and its surroundings during that period. In late June and July 1995 (Figure 3(e,f)) water of the same properties was limited to a comparatively small area above the summit. Due to the influence of the general warming of the upper water column in summer the core properties were eroded compared to spring 1994 but still clearly distinguishable from the warmer waters outside the bank area.

To illustrate the vertical structure and extent of the observed properties, Figure 4 shows the vertical distribution of potential temperature Θ (°C) and potential density σ_0 (kg m^{-3}) presented along the northernmost transect across Porcupine Bank based on the 1994 and 1995 CTD data. The measurements exhibit a remarkable vertical deformation of the temperature and density fields above the bank summit which is evident throughout the bank area at depths <400 m. The anomaly is characterized by an uplifting of isotherms and isopycnals generating strong horizontal temperature and density gradients along the flanks of the bank. This front-like structure separates a dome of cold and dense water above the summit from the warmer water masses outside the bank region. The intensity and amplitude of the temperature and density anomaly is marked by a pronounced variability associated with the different stratification conditions. In March/April 1994 (Figure 4(a,b)) the water column is weakly stratified due to enhanced mixing by strong storm events which crossed the area immediately before the sampling period. The uplifting of the 9.8°C isotherm and the 27.33 kg m^{-3} isopycnal, which are taken as an adequate reference for the anomaly, extends over the whole water column from the outer flanks to the sea surface. In April/May 1994 (Figure 4(c,d)), the strength of the stratification is increased by the development of the seasonal thermocline. As a consequence, the dome-like deformation of the reference isotherm and isopycnal is weakened and restricted to the inner bank area compared to the situation found in March/April 1994. In summer 1995 (Figure 4(e,f)) the seasonal thermocline is fully developed and the stratification is further intensified. At that time the dome is highly bottom-trapped and concentrated predominantly in the direct vicinity of the bank summit. From these observations it is suggested, that the

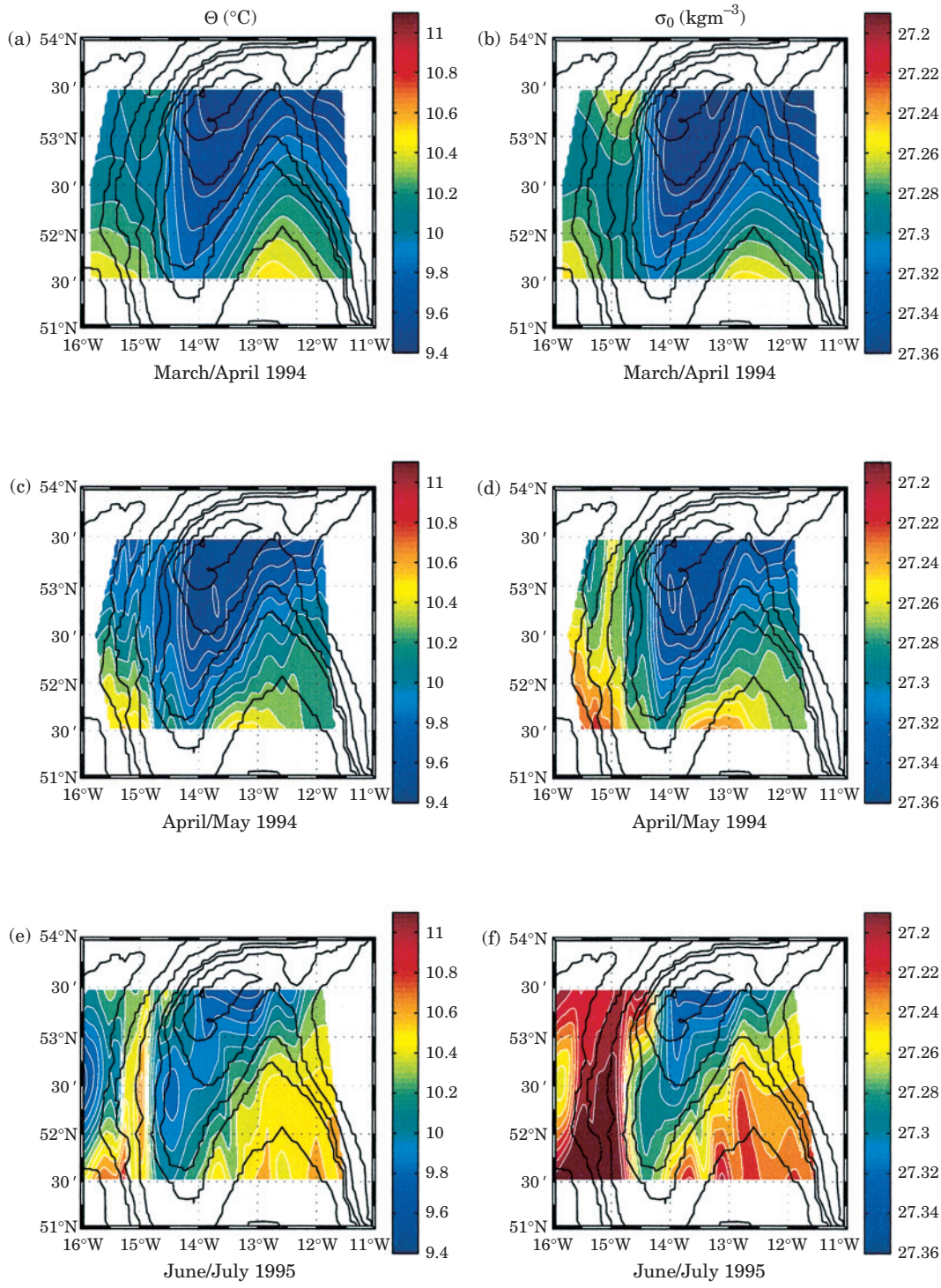

Figure 3. Horizontal distribution of potential temperature Θ (°C) and potential density σ_0 (kg m^{-3}) on the 180 dbar isobar during different observation periods in the Porcupine Bank area. The contour interval is 0.1°C and 0.01 kg m^{-3}, respectively.

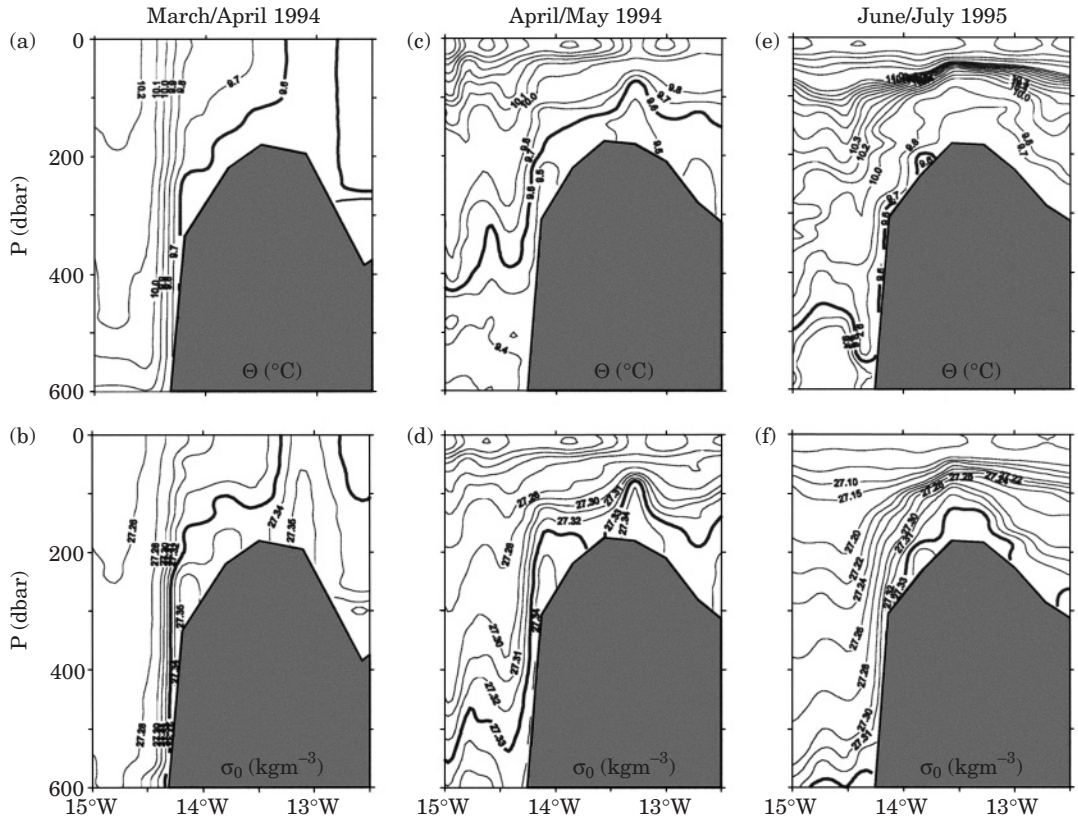

Figure 4. Vertical distribution of potential temperature Θ (°C) and potential density σ_0 (kg m^{-3}) in the top 600 dbar during different observation periods at 53.5°N across the central Porcupine Bank.

structure of the dome is strongly determined by the background stratification.

In order to shed light on the three-dimensional spatial structure of the doming, additional distributions of temperature and density are presented on two transects south of the bank summit during 1995 at 51.5°N (Figure 5(a,b)) and 52.5°N (Figure 5(c,d)). From these distributions it can be seen that the observed temperature and density doming above the central bank summit extends across the whole Porcupine Bank area. Because of the effect of the strong near surface stratification the compression and bottom trapping of the cold, dense dome is most pronounced above the shallow bank summit at 53.5°N (Figure 4(e,f)). In the deeper portions of the bank with water depths up to 500 m, the doming is almost unaffected but again does not intersect the thermocline (Figure 5(a–d)).

To elucidate the effect of the stratification on the intensity of the observed temperature and density doming above Porcupine Bank, NOAA/NASA AVHRR (Advanced Very High Resolution Radiometer) Oceans Pathfinder SST data were used to analyze monthly averages of the sea surface temperature distribution in the study area. The spatial resolution of the data is 54 km in both north–south and east–west directions. Figure 6 shows the SST distribution in selected months between January and June for the years 1994 and 1995. A distinct surface core of low temperature was not evident above the central bank area during the selected months in 1994 (Figure 6(a–d)). Nevertheless, lower surface temperatures in the Porcupine Bank area are enclosed by warmer water in the Porcupine Seabight and west of the bank indicating a cool surface region above the shallower parts of the Bank from January to April 1994 (Figure 6(a–c)). In June 1994 (Figure 6(d)) the tongue of cold water no longer exists as a result of enhanced surface warming.

In contrast to the surface temperature distribution during 1994, a distinct cold-core anomaly over the central bank is evident from January to April 1995 (Figure 6(e–g)). With progressive sea surface warming the core is eroded and no longer visible in summer 1995 (Figure 6(h)). The large discrepancies in the surface signature of the cold anomaly over Porcupine Bank between 1994 and 1995 can be attributed to an enhanced entrainment of cold coastal waters into the central bank area in 1994. The March/April 1994 CTD measurements show that storm events, which passed through the area

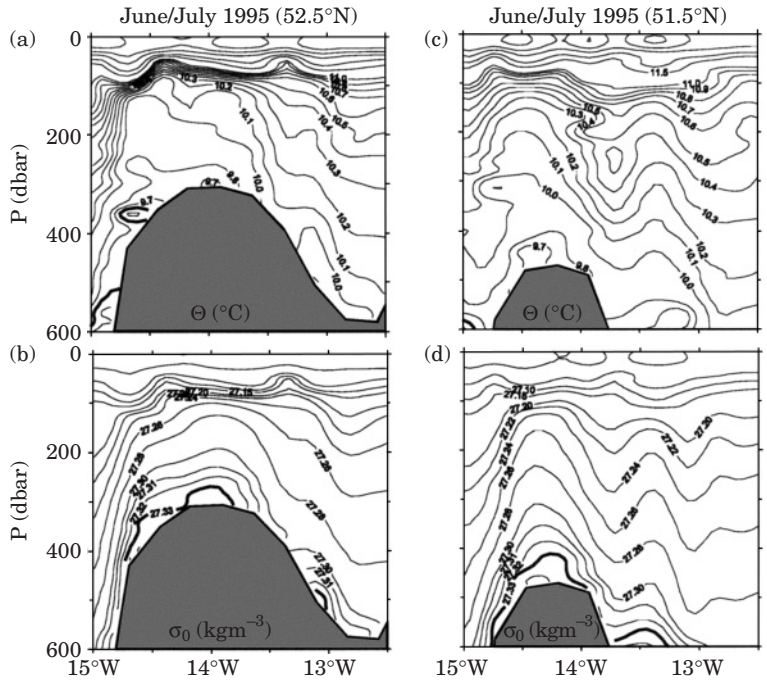

Figure 5. Vertical distribution of potential temperature Θ (°C) and potential density σ_0 (kg m^{-3}) in the top 600 dbar in June/July 1995 at 52.5°N and 51.5°N.

before sampling, are able to destroy the doming. Furthermore, observations by Huang *et al.* (1991) based on sequences of satellite images recorded between 1981 and 1987, reveal enhanced eddy formation associated with baroclinic instabilities at the Irish Shelf front. These instabilities are mainly due to the relative variation of the Shelf Current and the North Atlantic Current (Huang *et al.*, 1991). These results indicate that the existence and persistence of a distinct cold dome strongly depends on the near-surface stratification but may also be affected by the extent of eddy formation in the area.

Flow field

For an analysis of the bank-related flow dynamics current observations are available for the June/July 1995 field campaign only. The results of the vessel-mounted ADCP measurements carried out across the Porcupine Bank area along leg 2 (52.5°N and 53.5°N, see Figure 2) are presented in Figure 7. The tidally-corrected ADCP data are presented along 11 depth levels between 40 m and 240 m.

The current-field along both transects is dominated by an anti-cyclonic circulation, which is limited to a small area from the seamount summit to the upper flanks of the Bank. Along the northernmost transect at 53.5°N (Figure 7(a)) it extends over the whole water column below the mixed layer. The highest velocities are found along the upper flanks of the Bank decreasing substantially towards its summit and the adjacent deeper oceanic regions. The flow clearly follows isobaths and is oriented north-eastwards along the western flank and south-westward along the eastern flank of the central Porcupine Bank, respectively. From horizontally-averaged profiles of the north–south component of the ADCP velocities along the western and eastern upper flanks two prominent features can be distinguished at 53.5°N (Figure 7(c)): the flow is strongly bottom-intensified and asymmetric. To the west of the bank summit, a strong velocity shear is found within the mixed layer at depths <50 m. Below 60 m the flow weakens, but strengthens again towards the bottom with a maximum of 14 cm s^{-1}. A similar structure is found above the eastern flank. The vertical velocity shear is generally weaker. The amplitude varies between 15 cm s^{-1} within the wind-mixed layer and 20 cm s^{-1} near the bottom. Thus the anti-cyclonic vortex is substantially amplified on its eastern side.

A similar flow pattern can be observed at 52.5°N (Figure 7(b)). Below the thermocline the flow turns northwards along the western flank and southwards along the eastern flank respectively. The amplitude of the flow is generally weaker compared to the velocities found along the bank summit further north. To allow comparison with the flow characteristics at 53.5°N, corresponding horizontally-averaged profiles were generated for the north–south component of the ADCP

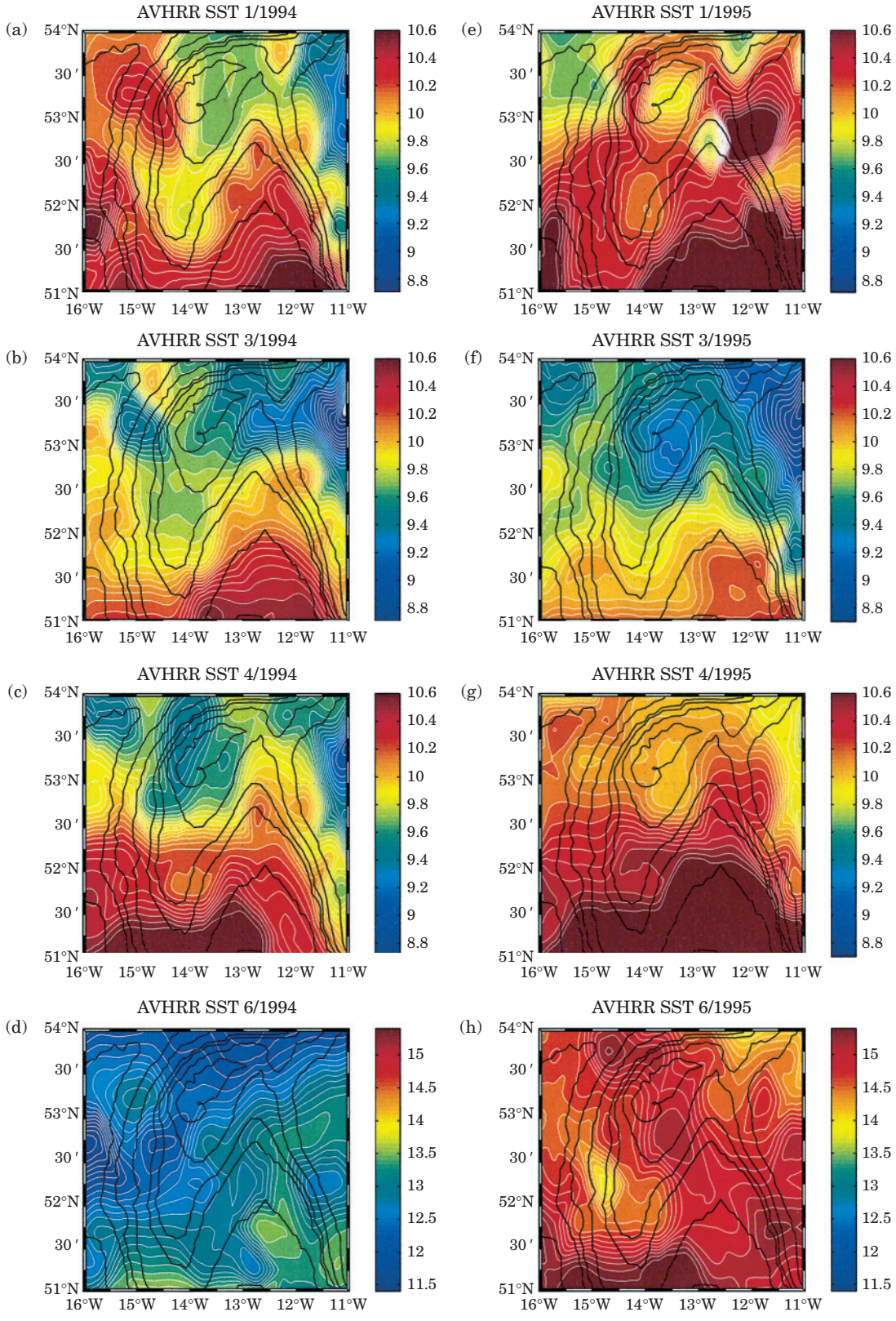

Figure 6. Monthly averages of the sea surface temperature (°C) derived from NOAA/NASA Oceans Pathfinder SST observations during different observation periods in 1994 and 1995 in the Porcupine Bank area. Colour shading is the same for each calendar month except for June 1994 and 1995. The contour interval is 0.05°C (January to April) and 0.1°C (June) respectively.

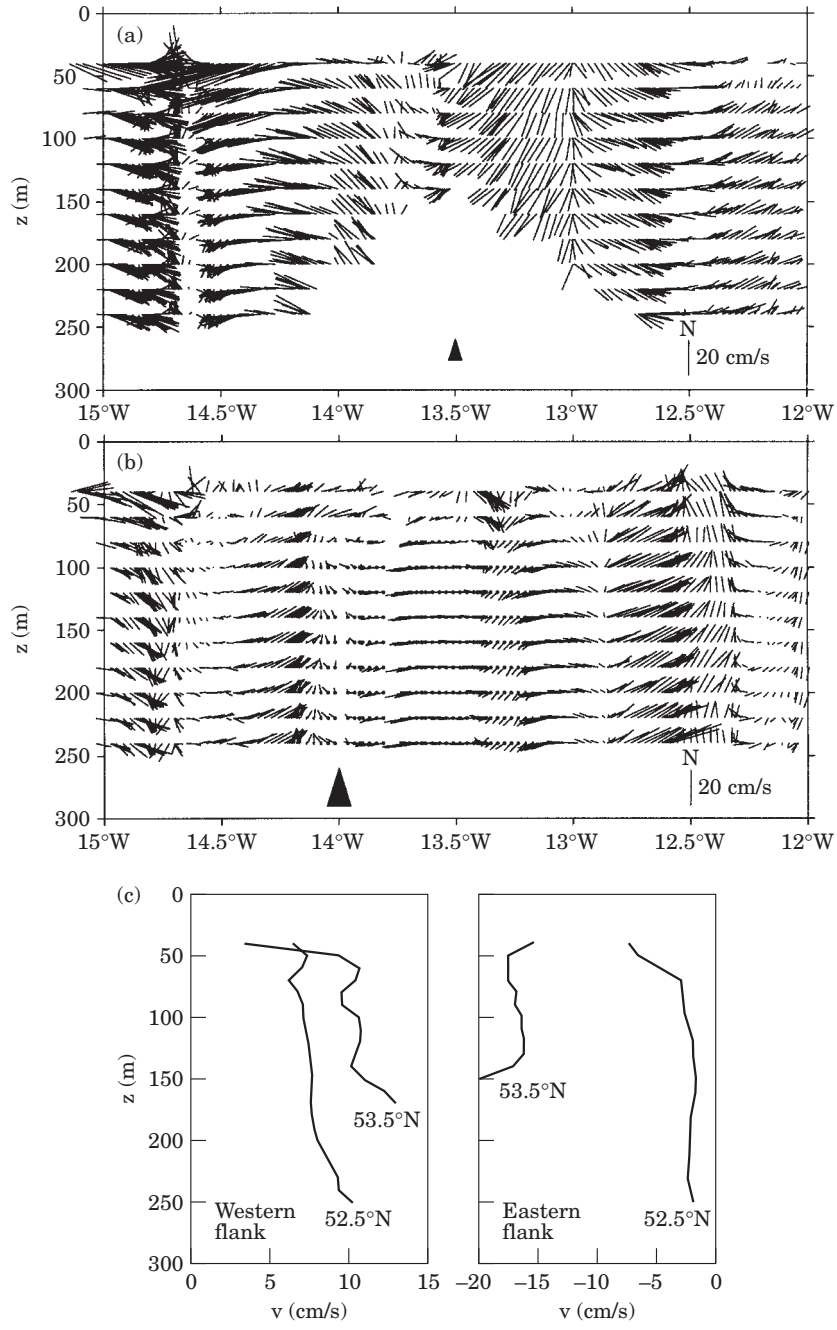

Figure 7. Tidally-corrected ADCP current field (cm s^{-1}) in the top 240 m across the Porcupine Bank based on the July 1995 measurements at 53.5°N (a) and 52.5°N (b). The filled triangle represents the position of the bank summit (see Figure 2). (c): Profiles of the north-south component (cm s^{-1}) of the ADCP velocities for the July measurements, horizontally averaged over the upper flanks of the Porcupine Bank at 52.5°N and 53.5°N.

velocities at this latitude (Figure 7(c)). The most striking differences are the reversed zonal asymmetry and the weakening of the flow. Along the western flank the current velocities are amplified to a maximum of 10 cm s^{-1}at the bottom, while maximum velocities of 3 cm s^{-1} are not exceeded along the eastern flank below 100 m depth.

Other strong signals in the flow pattern arise from a northward flow along the Irish shelf break which can be attributed to the eastern branch of the SEC and a

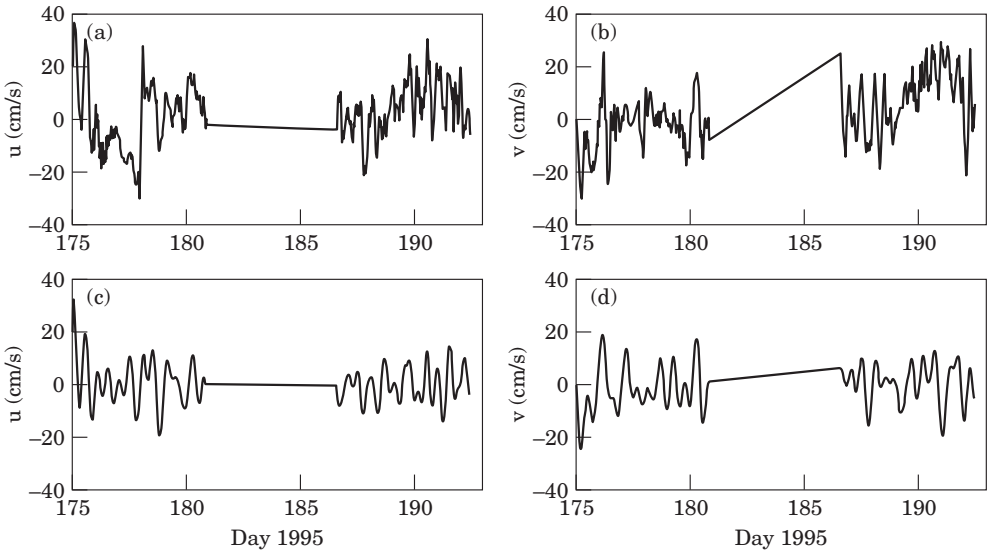

Figure 8. East-west (a) and north-south (b) components of the vertically-averaged total water velocity from the ADCP measurements. East–west (c) and north–south (d) components of the K_1 and M_2 tidal velocity from a least-square fit to the vertically-averaged total water velocity.

southward flow along the deeper portions of the Porcupine Bank between 14.5°W and 15°W which corresponds to a tongue of relatively cold and low saline water (Mohn, 1999).

Tidal analysis

Recent observational and numerical studies at isolated seamounts in a stratified ocean (e.g. Chapman and Haidvogel, 1992; Kunze and Toole, 1997; Beckmann and Haidvogel, 1997) identified two principal physical mechanisms which can generate the currents observed structure. These are either the formation of a "Taylor cap" by a steady impinging flow or the non-linear flow rectification, through the generation of seamount-trapped waves, by resonance with diurnal tides. Both mechanisms lead to a closed anti-cyclonic circulation around seamounts. The relative importance of these mechanisms for the Porcupine Bank cannot be deduced from the available data base alone.

The northward-flowing SEC (Shelf-Edge Current) forms a steady inflow to the Porcupine Bank area, varying seasonally in strength with a winter maximum of 20 cm s^{-1} (Huthnance and Gould, 1989; Pingree *et al.*, 1999) and acts as one possible source for the observed anticyclonic re-circulation over Porcupine Bank. To estimate the influence of tidally-induced flow rectification, the tidal analysis from the ADCP measurements at Porcupine Bank are presented in Figure 8 and Figure 9(a). Uncertainties in the determination of the tidal currents arise mainly from the lack of information over one full tidal cycle and ADCP measurement errors. Additionally, small-scale spatial variability can be misinterpreted as tidal motion. Hence Candela's method (Candela *et al.*, 1990) must be recognized as a first-order estimate. Figure 8 presents the vertically-averaged components of the total water velocity (a, b) and the amplitude of the main tidal constituents M_2 and K_1 (c, d). In most regions of the sampling area the amplitude of the tidal currents does not exceed 10 cm s^{-1}. A large portion of the tidal motion on the total velocity can be observed at the Irish shelf (year days 175–177 and 191–193) and in the shallower areas of the Porcupine Bank (year days 180–181 and 187–188).

For the diurnal and semi-diurnal constituents K_1 and M_2, the tidal flow is mainly north–south. A relevant amplification of the diurnal tidal currents near the bank can be observed along its eastern flank. At 53.5°N diurnal tidal currents up to 10 cm s^{-1} were observed over the bank (Figure 9(b)) relative to typical diurnal tidal velocities of 1 cm s^{-1} in the Northeast Atlantic (Huthnance, 1974). Further south at 52.5°N, diurnal tidal currents are slightly weaker with maximum velocities of 8 cm s^{-1} above the eastern flank (Figure 9(b)). A corresponding amplification factor of the semi-diurnal constituent was not observed (Figure 9(a)). On both transects maximum currents do not exceed 8 cm s^{-1} over the Bank in contrast to approximately 5 cm s^{-1} in the deep ocean regions to its west (White *et al.*, 1997).

To verify these results the global inverse tidal model TPXO.5.1 with a 0.5 resolution was run for the 1995 observation period at the Porcupine Bank area. For details on the computational methods in the model see Egbert *et al.* (1994). Tidal-current ellipses for the main

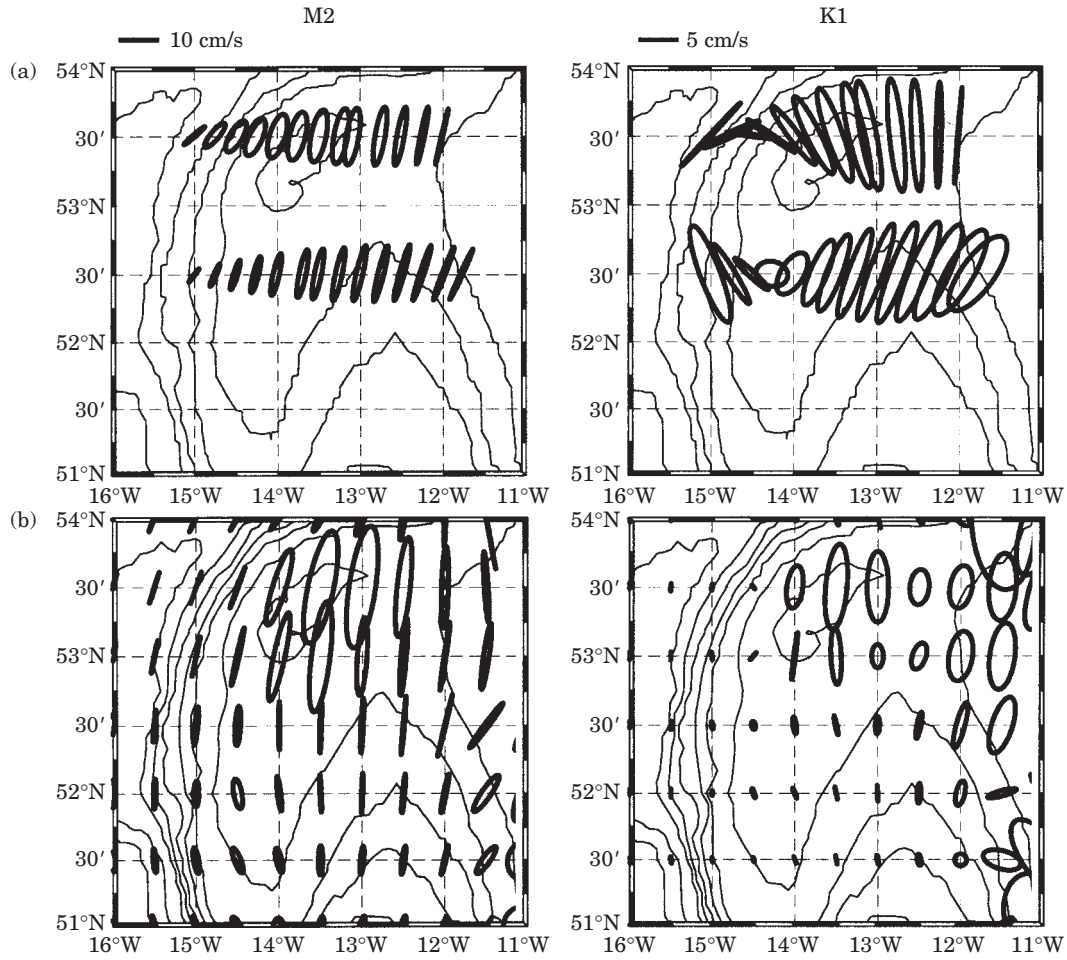

Figure 9. Current ellipses of the K_1 and M_2 tidal constituents in the Porcupine Bank area from the ADCP measurements (a) and the TPOX.5.1 inverse tidal model (b).

frequencies M_2 and K_1 are presented in Figure 9(c) and (d). There is a qualitative correspondence between the observations and model results for the semi-diurnal constituent. The tidal ellipse is oriented north–south with a near-bank maximum of 8 cm s^{-1} at 53.5°N. This is an eightfold amplification relative to diurnal tidal currents in the deep ocean regions to the west (Figure 9(d)). A continuous decrease can be observed to the south where large discrepancies between model results and the observations are evident at 52.5°N. The K_1 tidal amplitude in the model does not exceed 2 cm s^{-1} and no relevant amplification is found (Figure 9(b)). Taking into account the uncertainties in the de-tiding of the ADCP data it is probable that the observed ADCP diurnal tides are strongly overestimated in that area.

A close correspondence between model results and observations is evident for the M_2 constituent. Compared to the diurnal signal, the semi-diurnal amplification over the central Porcupine Bank area in the model is weak, i.e. an amplification factor of 3 relative to the deep Northeast Atlantic, which is similar to the measurements. Nonetheless the semi-diurnal tidal currents derived from the measurements are underestimated over the central bank area at 53.5°N,where the model predicts maximum velocities of the order of 15 cm s^{-1}.

Discussion

From the hydrographic measurements there is clear evidence of a substantial deformation of the mass field in the vicinity of Porcupine Bank. It is marked by an uplifting of isotherms and isopycnals with cold, dense water lying above the Bank's summit. In the case of weak stratification (March/April 1994) the doming is transposed to an almost column-like structure. Moderate and strong stratification conditions, as observed in

April/May 1994 and June/July 1995, cause enhanced bottom-trapping of the temperature and density doming. Monthly-averaged satellite SST distributions from January to June during 1994 and 1995 were analyzed to investigate the sea-surface signature of the cold core. During the 1994 observation period a distinct cold surface core was not evident. A cool surface region above the shallower portions of the Bank enclosed by warmer water in its deep ocean surroundings was observed instead. In 1995, the sea-surface temperature distribution was marked by a prominent cold-core anomaly from January to April. It became colder from January to March, warmed up again to April and finally was eroded in June due to increasing sea-surface warming. This indicates that the doming above Porcupine Bank is a quasi-permanent feature during late winter and early spring. With increasing strength of the near-surface stratification in late spring and summer the doming is restricted to depths immediately above the bank summit.

The flow dynamics associated with the deformation of the mass field under strong stratification conditions were presented by tidally-corrected residual currents derived from vessel-mounted ADCP measurements carried out in June/July 1995 along two transects across the Porcupine Bank area. The flow field is marked by an anti-cyclonic circulation along the upper flanks of the bank. The highest velocities are found along the flanks of the bank summit at 53.5°N with a substantial flow amplification along the eastern flank, while at 52.5°N flow amplification occurs along the western flank. The vertical structure of the flow is generally marked by a bottom-intensification below the thermocline.

There are two fundamentally different mechanisms generating closed anti-cyclonic time-mean flows at seamounts: "Taylor cap" formation by steady currents and tidal rectification respectively. A "Taylor cap" re-circulation is found in areas where a persistent flow encounters a topographic obstacle, e.g. a coastal boundary current impinging on a bank near a shelf edge (Gjevik and Moe, 1993). The corresponding "Taylor cap" flow is strongly asymmetric with substantially enhanced velocities on the left side (northern hemisphere) of the obstacle looking downstream (Chapman and Haidvogel, 1992). Tidal rectification, on the other hand, leads to a more symmetric re-circulation and is the principal mechanism for the generation of closed circulation cells at seamounts in areas with weak or variable far-field currents (Beckmann, 1999). Strong diurnal tidal amplification was observed by Huthnance (1974) at Rockall Bank and Hunkins (1986) at the Yermak Plateau in the Arctic Ocean.

Which of the two is most important at Porcupine Bank cannot be determined from the present observations alone. However the characteristics of the observed flow pattern (e.g. symmetric or asymmetric re-circulation, tidal amplification) give some indication of the generating forces. To estimate the tidal influence on the observed residual circulation at Porcupine Bank, a tidal analysis of the summer 1995 ADCP data was carried out and compared with the results of the global inverse tidal model TPXO5.1 (Egbert *et al.*, 1994). Despite the observed quantitative discrepancies both tidal model and observations show a strong amplification of the diurnal tidal current over the central Bank area. This indicates that tidal rectification may play the major role in generating the observed anti-cyclonic residual circulation above the bank summit. The results of the tidal analysis agree with the results of numerical model studies (Mohn and Beckmann, 2001) in which the diurnal tidal rectification was identified as the dominant mechanism for generating anti-cyclonic currents over central Porcupine Bank.

The consequences of a closed re-circulation phenomenon at Porcupine Bank for the transport of pelagic eggs and larvae is likely to be substantial. The results of this study corroborate earlier investigations by Bartsch and Coombs (1997, 2001) based on numerical dispersion simulations which show that Porcupine Bank is a retention area for the eggs and larvae of blue whiting (*Micromesistius poutassou* (Risso)) and mackerel (*Scomber scombrus*). Simulations were carried out for dispersion scenarios in March/April 1995 and May/June 1995 respectively. Original tracer concentrations over Porcupine Bank at the beginning of the simulations increased by a factor of up to 3 by the end of the simulations two months later (Bartsch and Coombs, 2001). In general, eggs and larvae of any species originating at or transported to Porcupine Bank will be trapped over the bank. Under certain circumstances (e.g. storm events) eggs and larvae can leave the area. The degree of retention, i.e. the fraction of particles remaining in the Porcupine Bank area, is dependent on the wind-stress field as well as the background flow impinging on the bank. Studies on the stability and stationarity of a Taylor column circulation relative to changes of the atmospheric forcing are currently under investigation. White *et al.* (1998) found an enrichment of inorganic nutrients within the cold, dense dome over Porcupine Bank and little exchange with adjacent water masses. They also acknowledge the possibility of a retention system with good conditions for species settlement.

To clarify the dynamics and the generating mechanisms of the flow field at Porcupine Bank further repeated and systematic field investigations are needed. Furthermore, numerical studies like those carried out by Beckmann and Haidvogel (1997) and Mohn and Beckmann (2001) can help to shed light on these factors and on whether the re-circulation cell over Porcupine Bank is a quasi-permanent feature.

Acknowledgements

The authors wish to thank the master, crew and scientists on RV "Valdivia" and RV "Heincke" for their great support during the measurements. This study was funded by the EU/AIR (contract no. AIR2-CT93-1105) and the Deutsche Forschungsgemeinschaft (DFG Me 487/37-1). We would also like to thank all colleagues, who were involved in this investigation for helpful discussions.

References

Bartsch, J., and Coombs, S. 1997. A numerical model of the dispersion of blue whiting larvae, *Micromesistius poutassou* (Risso), in the eastern North Atlantic. Fisheries Oceanography, 6(3): 141–154.

Bartsch, J., and Coombs, S. 2001. An individual-based growth and transport model of the early life-history stages of mackerel (*Scomber scombrus*) in the eastern North Atlantic. Ecological Modelling, 138(1-3): 127–141.

Beckmann, A. 1995. Numerical modelling of time-mean flow at isolated seamounts. *In* Topographic effects in the ocean, Proceedings Hawaiian Winter Workshop, January 17–20 1995, University of Hawaii at Manoa, 57–66.

Beckmann, A. 1999. Dynamical processes at isolated seamounts. Habil. thesis, Carl-von-Ossietzky University Oldenburg. 87 pp.

Beckmann, A., and Haidvogel, D. B. 1997. Numerical simulation of flow at Fieberling Guyot. Journal of Geophysical Research, 102: 5595–5613.

Bersch, M. 1995. On the circulation of the north-eastern North Atlantic. Deep-Sea Research, 42: 1583–1607.

Boehlert, G. W. 1988. Current-topography interactions at mid-ocean seamounts and the impact on pelagic ecosystems. GeoJournal, 16: 45–52.

Brink, K. H. 1990. On the generation of seamount-trapped waves. Deep-Sea Research, 37: 1569–1582.

Candela, J., Beardsley, R. C., and Limeburner, R. 1990. Removing tides from ship-mounted ADCP data, with application to the Yellow Sea. In Proceedings of the IEEE fourth working conference on current measurements, Institute of Electrical and Electronics Engineers, New York, 859–865.

Chapman, D. C., and Haidvogel, D. B. 1992. Formation of Taylor caps over a tall, isolated seamount in a stratified ocean. Geophysical and Astrophysical Fluid Dynamics, 64: 31–65.

Dooley, H. D. 1984. Aspects of oceanographic variability on Scottish fishing grounds. Ph.D. thesis, University of Aberdeen, 156 pp.

Egbert, G. D., Bennett, H. A. F., and Foreman, M. G. G. 1994. TOPEX/POSEIDON tides estimated using a global inverse model. Journal of Geophysical Research, 99: 24821–24852.

Firing, E., Ranada, J., and Caldwell, P. 1995. Processing ADCP data with the CODAS software system version 3.1. User's manual. Joint Institute for Marine and Atmospheric Research, University of Hawaii.

Genin, A., Dayton, P. K., Lonsdale, P. F., and Spiess, F. N. 1986. Corals on seamount peaks provide evidence of current acceleration over deep-sea topography. Nature, 322: 59–61.

Genin, A., Noble, M., and Lonsdale, P. F. 1989. Tidal currents and anti-cyclonic motions on two North Pacific seamounts. Deep-Sea Research, 36(12): 1803–1815.

Gjevik, B., and Moe, H. 1994. Steady and transient flows around banks located near a shelf edge. Continental Shelf Research, 14(12): 1389–1409.

Huang, W. G., Cracknell, A. P., Vaughan, R. A., and Davies, P. A. 1991. A satellite and field view of the Irish Shelf front. Continental Shelf Research, 11(6): 543–562.

Hunkins, K. 1986. Anomalous diurnal tidal currents on the Yermak Plateau. Journal of Marine Research, 44: 51–69.

Huthnance, J. M. 1974. On the diurnal tidal currents over Rockall Bank. Deep-Sea Research, 21: 23–35.

Huthnance, J. M., and Gould, W. J. 1989. On the Northeast Atlantic slope current. *In* Poleward flows along eastern ocean boundaries, pp. 76–81. Ed. by S. Neshiba, C. N. K. Mooers, R. L. Smith, and R. T. Barber. Springer Verlag, Berlin. 374 pp.

Kunze, E., and Toole, J. M. 1997. Tidally driven vorticity, diurnal shear and turbulence atop Fieberling Guyot. Journal of Physical Oceanography, 27: 2663–2693.

Loder, J. W., Ross, C. K., and Smith, P. C. 1988. A space- and timescale characterization of circulation and mixing over submarine banks, with application to the north-western Atlantic continental shelf. Canadian Journal of Fisheries and Aquatic Sciences, 45: 1860–1885.

Meincke, J. 1971. Der Einfluss der Grossen Meteorbank auf Schichtung und Zirkulation der ozeanischen Deckschicht. (The influence of the Great Meteor seamount on stratification and circulation within the mixed layer). Meteor Forschungsergebnisse, A(9): 67–94.

Mohn, C. 1999. Wassermassen und Strömungen im Bereich des europäischen Kontinentalrandes westlich von Irland. (Water masses and currents at the European shelf edge west of Ireland). Ph.D. thesis, Universität Hamburg, Fachbereich Geowissenschaften, pp. 133.

Mohn, C., and Beckmann, A. 2001. Numerical studies on flow amplification at a shelfbreak bank, with application to Porcupine Bank. Continental Shelf Research, in press.

Pingree, R., and LeCann, B. 1990. Celtic and Armorican slope and shelf residual currents. Progress in Oceanography, 23: 303–338.

Pingree, R., Sinha, B., and Griffiths, C.R. 1999. Seasonality of the European slope current (Goban Spur) and ocean margin exchange. Continental Shelf Research, 19: 929–975.

Rogers, A. D. 1994. The biology of seamounts. Advances of Marine Biology, 30: 305–350.

White, M., Raine, R., and Bowyer, P. 1997. Slope current dynamics and variability west of Ireland. In OMEX II-I final report.

White, M., Mohn, C., and Orren, M. 1998. Nutrient distributions across the Porcupine Bank. ICES Journal of Marine Science, 55: 1082–1094.